P-Vector Method for Determining Absolute Velocity From Hydrographic Data

PAPER

Peter C. Chu
Department of Oceanography
Naval Postgraduate School
Monterey, California

ABSTRACT

Several major techniques (Stommel-Schott method, Wunsch method, and Bernoulli method) that have been developed to quantitatively estimate the geostrophic velocity at the reference level, have the same order of dynamical sophistication (geostrophy, hydrostatic, and density conservation.) From a technical point of view, the Stommel-Schott method is an overdetermined system (the number of equations is much larger than the number of variables), however, the Wunsch method is an underdetermined system (the number of equations is much smaller than the number of variables). Based on the same dynamical and thermodynamical framework, a simple, well-posed system (P-vector method) is proposed in this study. Consistent with geostrophy, the system is assumed non-dissipative. The conservation of mass and potential vorticity leads to the condition that the velocity vector is perpendicular to both density (ρ) and potential vorticity ($q = f\partial\rho/\partial z$) gradients, and that the velocity can be represented as $V(x, y, z) = r(x, y, z)\boldsymbol{P}(x, y, z)$, where $\boldsymbol{P} = (\nabla\rho \times \nabla q)/|\nabla\rho \times \nabla q|$. The unit vector, $\boldsymbol{P}$, is computed from the density field, and the parameter $r(x, y, z)$ is determined by the thermal-wind relation. Furthermore, an error reduction scheme is also proposed in this study.

INTRODUCTION

The physical base for calculating geostrophic velocity from hydrographic data is the integral form of the thermal wind relation

$$u = u_0 + \frac{g}{f\rho_0}\int_{z_{ref}}^{z} \frac{\partial\rho}{\partial y}\,dz' \tag{1a}$$

$$v = v_0 - \frac{g}{f\rho_0}\int_{z_{ref}}^{z} \frac{\partial\rho}{\partial x}\,dz' \tag{1b}$$

where (u, v), (u_0, v_0) are the geostrophic velocity at any depth z and at a reference level z_{ref}, g is the earth gravitational acceleration, ρ is the water density, and ρ_0 is the characteristic value of the density. Here, the Boussinesq approximation has been used. The hydrographic data only determine the baroclinic geostrophic current, i.e., the second term on the right hand side of (1). The reference velocity (u_0, v_0) still needs to be determined. Two techniques, the Stommel-Scott method (hereafter referred as SS method) and the Wunsch method (hereafter referred as CW method), have been developed to determine the reference velocity (u_0, v_0). Furthermore, the Bernoulli method (Killworth 1985) has been formulated to determine the reference Bernoulli function, B, and in turn to compute the pressure field (geostrophic velocity.) The SS method (usually called the β -spiral method) is to use the conservation of mass, density, and vorticity to estimate reference velocities and diffusivities of heat, salt, and potential vorticity (e.g., Stommel and Schott 1977; Schott and Stommel 1978; Olbers et al. 1985). The CW method (usually called the inverse method) is to estimate the reference velocity by balancing the fluxes of water mass and several tracers into and out of a closed region (e.g., Wunsch 1978; Wunsch and Grant 1982). Both methods are based on the same order of dynamical sophistication and differ from implicit assumptions about the scales of oceanic variability and different definitions of the smooth field to which the dynamic model pertains (Davis 1978). From a technical point of view, the SS and Bernoulli methods are overdetermined systems (the number of equations is larger than the number of unknowns), however, the CW method is an underdetermined system (the number of equations is less than the number of unknowns.) Can we design a well-posed system (the number of equations equals to the number of unknowns) and still keep the same dynamical sophistication as the SS, CW, and Bernoulli methods? To answer this question, we should first investigate the conservation principles associated with these methods.

CONSERVATION PRINCIPLES

As pointed out by Wunsch and Grant (1982), in determining large-scale circulation from hydrographic data we can be reasonably confident on the assumptions of geostrophic balance, mass conservation, and no major cross-isopycnal mixing (except when water masses are in contact with the atmosphere). The potential density of each fluid element, ρ, would be conserved, i.e.,

$$V \cdot \nabla\rho = 0 \tag{2}$$

where

$$\nabla \equiv \boldsymbol{i}\frac{\partial}{\partial x} + \boldsymbol{j}\frac{\partial}{\partial y} + \boldsymbol{k}\frac{\partial}{\partial z} \tag{3}$$

Here $V = (u, v, w)$, is the three dimensional velocity, (x, y, z) is the coordinate, and z is positive upward. At the undisturbed ocean surface, $z = 0$. The potential density (potential temperature) is the density (temperature) a parcel of water would have if brought adiabatically from its initial state to the standard pressure of 1000

mb. After obtaining the temperature and salinity data, we compute the potential temperature (Θ) using the Bryden formula (Bryden 1973) and the potential density (ρ) using the equation of state (the temperature be replaced by the potential temperature) defined by the Joint Panel on Oceanographic Tables and Standards (UNESCO 1981). Differentiating (2) with respect to z, using the geostrophic and hydrostatic balance, and including the latitudinal variation of the Coriolis parameter, we can obtain the conservation of potential vorticity equation:

$$\boldsymbol{V} \cdot \nabla q = 0,\ q \equiv f \frac{\partial \rho}{\partial z} \tag{4}$$

where $f = 2\Omega \sin \phi$, is the Coriolis parameter, $\Omega = 7.292 \times 10^{-5} s^{-1}$, is the angular speed of earth rotation. Use of $f\partial\rho/\partial z$ may induce a small but systematic error into estimation of potential vorticity (Needler 1985). The vector $\boldsymbol{V}$ is perpendicular to both $\nabla\rho$ and ∇q, therefore,

$$\boldsymbol{V} \sim \nabla q \times \nabla \rho \tag{5}$$

Pedlosky (1986) pointed out that the three-dimensional velocity field can be determined from knowledge of the density field unless the potential vorticity and density surfaces coincide.

FIGURE 1 The absolute velocity and the intersection of surfaces of ρ and q.

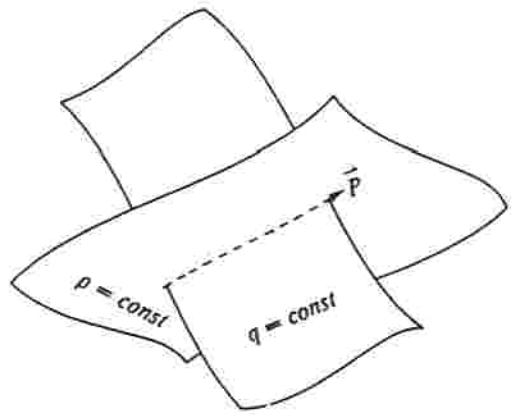

TABLE 1 The vertical resolution of the Levitus climatological data set

k	z-level (m)	k	z-level (m)	k	z-level (m)	k	z-level (m)
1	0	10	−200	19	−1000	28	−3000
2	−10	11	−250	20	−1100	29	−3500
3	−20	12	−300	21	−1200	30	−4000
4	−30	13	−400	22	−1300	31	−4500
5	−50	14	−500	23	−1400	32	−5000
6	−75	15	−600	24	−1500	33	−5500
7	−100	16	−700	25	−1750		
8	−125	17	−800	26	−2000		
9	−150	18	−900	27	−2500		

He also credited Stommel and Schott (1977) for bringing up the fact that the constant of integration of the thermal wind equations is determined if

$$\nabla q \times \nabla \rho \neq 0 \tag{6}$$

Killworth (1986) emphasized the importance of using (ρ, q) space rather than (T, S) space for determining absolute velocities. Following these ideas and taking a more practical approach, a new and simple method can be constructed by introducing a P-Vector field to determine velocity field by density field.

P VECTOR FIELD

Under the condition (6), a unit vector $\boldsymbol{P}$

$$\boldsymbol{P} = \frac{\nabla q \times \nabla \rho}{|\nabla q \times \nabla \rho|} \tag{7}$$

does exist and is determined by the density field only. The P-vector lies on the intersection of the constant potential density and potential vorticity surfaces (Figure 1). Therefore, (6) is the condition (both necessary and sufficient) for the existence of the P vector.

Climatological $\boldsymbol{P}$ field in the North Atlantic Ocean was constructed from the climatological mean potential density field (ρ) which was computed from the Levitus climatological mean temperature and salinity fields (Levitus 1982). The Levitus data has $1° \times 1°$ horizontal resolution, and 33 vertical levels (Table 1). We use the finite difference to compute the vertical and horizontal derivatives. The horizontal grid is $1° \times 1°$,

$$\Delta x = \frac{2\pi a \cos\phi}{360},\ \Delta y = \frac{2\pi a}{360},$$

and the vertical grid is the difference between the two vertical levels as indicated in Table 1,

$$\Delta z_k = z(k) - z(k+1).$$

Here, ϕ and a are the latitude and earth radius, respectively. Although the unit vector, $\boldsymbol{P}$, only carries partial information about the velocity field, it is rather surprising that the horizontal component, $\boldsymbol{P}_h = (P_x, P_y)$, catches the most important features of the North Atlantic general circulation. For example, at the 150 m depth $\boldsymbol{P}_h$ (Figure 2) resembles both the classical (Figure 3) and recent (e.g, Schmitz and McCartney 1993) views of the North Atlantic circulation quite well: (1) anticyclonic subtropical gyre in the western part of the ocean between 20°-45° N, (2) recirculation cell on the western side (west of 40° W) of the subtropical gyre, (3) cyclonic-anticyclonic dipole in the area (30° W-10° W, 30° N); and (4) high latitude cyclonic gyre (50°-60° N, 20° W-50° W).

Comparing (7) with (5), we obtain a relationship between velocity and P fields:

$$V = r(x, y, z)P \tag{8}$$

where $r(x, y, z)$ is a proportionality. Applying the thermal wind relation to any two different depths z_k and z_m, a set of algebraic equations for determining the parameter is obtained:

$$r^{(k)}P_x^{(k)} - r^{(m)}P_x^{(m)} = \Delta u_{km} \tag{9a}$$

$$r^{(k)}P_y^{(k)} - r^{(m)}P_y^{(m)} = \Delta v_{km} \tag{9b}$$

which are linear algebraic equations for $r^{(k)}$ and $r^{(m)}$. Here

$$r^{(i)} = r(x, y, z_i),$$

and

$$\Delta u_{km} \equiv \frac{g}{f\rho_0}\int_{z_m}^{z_k}\frac{\partial \rho}{\partial y}\,dz' \tag{10a}$$

$$\Delta v_{km} \equiv -\frac{g}{f\rho_0}\int_{z_m}^{z_k}\frac{\partial \rho}{\partial x}\,dz' \tag{10b}$$

The integrations in (10a) and (10b) were computed in this paper by the trapezoidal rule,

$$\int_{z_m}^{z_k} f(z)dz = \frac{1}{2}\sum_{j=m}^{k-1}[f(z_j) + f(z_{j+1})](z_j - z_{j+1}). \tag{11}$$

If the determinant

$$\begin{vmatrix} P_x^{(k)} & P_x^{(m)} \\ P_y^{(k)} & P_y^{(m)} \end{vmatrix} \neq 0, \tag{12a}$$

the algebraic equations (9) and (10) have definite solutions for $r^{(k)}$ $(m \neq k)$:

$$r^{(k)} = \frac{\begin{vmatrix} \Delta u_{km} & P_x^{(m)} \\ \Delta v_{km} & P_y^{(m)} \end{vmatrix}}{\begin{vmatrix} P_x^{(k)} & P_x^{(m)} \\ P_y^{(k)} & P_y^{(m)} \end{vmatrix}} \tag{12b}$$

As soon as $r^{(k)}$ is obtained, the absolute velocity field can be computed by (8).

SOURCES OF ERRORS OF THE P-VECTOR METHOD

For a given level, $z = z_k$, there are (N-1) sets (m = 1, 2, . . .k−1, k+1, . . .N) of equations (9a,b) for computing $r^{(k)}$. Here, N is the number of total levels in the density field. All the (N-1) sets of equations are compatible under the thermal wind constraint and should provide the same solution. However, due to errors in measurements (instrumentation errors) and computations (truncation errors), the parameter $r^{(k)}$ may vary with m. The error estimation and elimination of the P-vector method will be discussed in future papers.

FIGURE 2 North Atlantic Ocean P field computed from the Levitus temperature and salinity climatology at 150m.

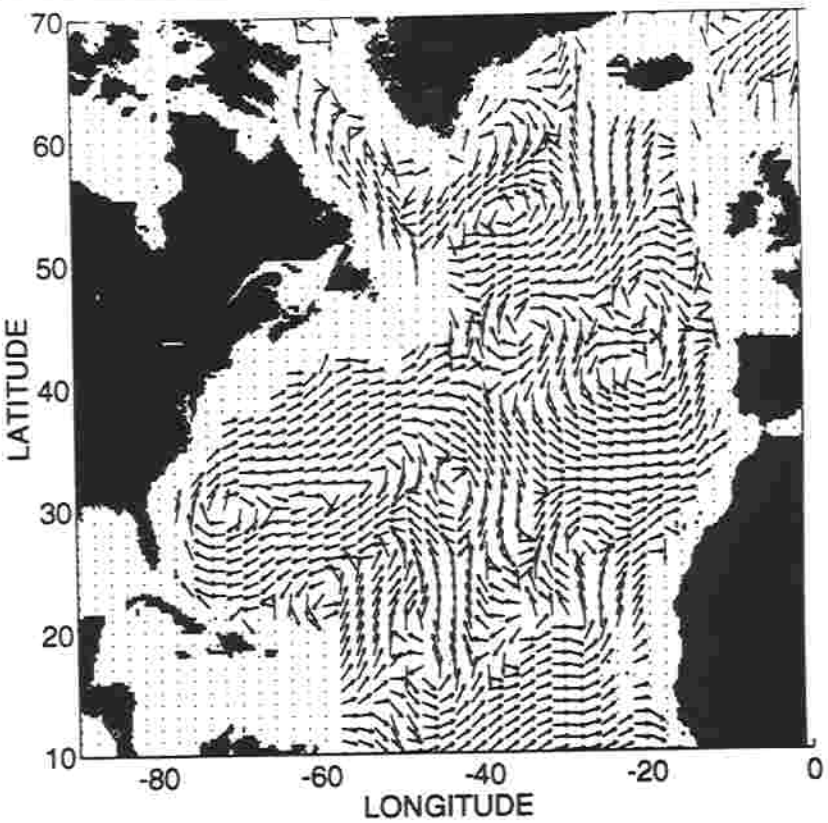

FIGURE 3 Classical view of streamline pattern in North Atlantic Ocean (from Iselin 1936).

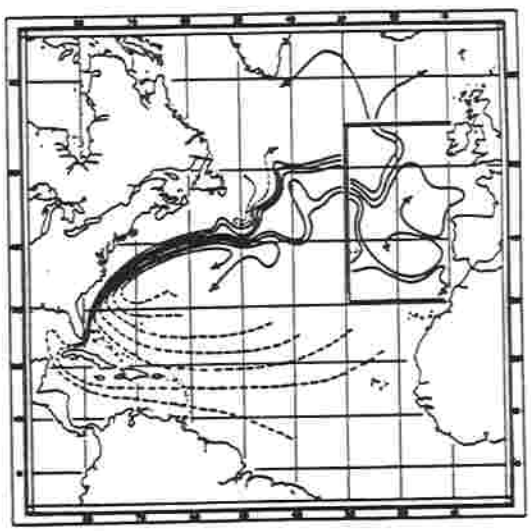

To obtain a good solution, we should first understand the physical significance of the P-vector. Consider the P-vector at two different levels, $z = z_m$, and $z = z_k$ (Figure 4a), and define α to be the angle between P_k and the x-axis (Figure 4b),

$$P_x = \cos\alpha,\ P_y = \sin\alpha. \tag{13}$$

The determinant (12a) becomes

$$\begin{vmatrix} P_x^{(k)} & P_x^{(m)} \\ P_y^{(k)} & P_y^{(m)} \end{vmatrix} = \sin(\alpha_{km}) \tag{14}$$

where

$$\alpha_{km} \equiv \alpha^{(k)} - \alpha^{(m)},$$

indicating the β spiral turning angle between two levels, $z^{(k)}$ and $z^{(m)}$.

MAXIMUM TURNING ANGLE PRINCIPLE

The validity of the β spiral method proposed by Stommel and Schott (1977) depends on the turning angle α_{km}. If α_{km} is close to 0 (almost no turning angle), the β spiral method fails to determine the absolute velocity from the hydrographic data.

Different from the β spiral method, the P-vector method has (N-1) choices (degree of freedom) for picking a level (z_m) for the computation. Theoretically, all the (N-1) sets of equations (9) are equivalent. Therefore, we have freedom to ignore those levels leading to very small turning angles. To assure the best solution, we adopt a maximum turning angle principle to get the level z_{m_k}

$$|\sin(\alpha_{km_k})| = \max_{m \neq k} |\sin(\alpha_{km})| \tag{15}$$

for computing $r^{(k)}$ in (9) and in turn, determining the absolute velocity $V^{(0)}(x, y, z_k)$ at the level z_k. The horizontal velocity field $V_h^{(0)}$ at the 500 m depth (Figure 5a) displays a circulation pattern in the main thermocline very similar to that obtained by Olbers et al. (1985) using SS method (Figure 6). The circulation pattern is dominated by a broad Gulf Stream leaving the North American coast at about 35° N, turning towards the east at 38° N, 60° W to a branching point at about 40° N, 40° W, splitting into two branches. The northern branch moves water northeastward until reaching 50° N and deflects towards north at 50° N, 15-30° W. The width of this branch increases northeastward from 700 km at 40° N, 50° W to nearly 1500 km in the northeast Atlantic at 50-60° N, 15-30° W.

The southern branch moves water southeastward between 30° N and 35° N toward Gilbratar, and feeds into the subtropical gyre. Our solution also shows a tight recirculation cell on the western side of the subtropical gyre which was depicted in earlier research (e.g., Stommel et al. 1978; Reid 1978; Olbers et al. 1985). Furthermore, a northern cyclonic gyre exists, but is much weaker than the subtropical gyre.

Figure 5b shows the vertical velocity at 500 m depth, computed by

$$w = r(x, y, z)P_z(x, y, z).$$

In the vast areas of the North Atlantic Ocean, the vertical velocity is quite weak (less than 1 m/day) and noisy except in a very small area south of Iceland, where a very strong downward velocity (> 4 m/day) is found. This coincides with the strong downward branch of the global conveyor belt (Broecker 1991). We also see that in the subtropical gyre, the water is usually downwelling. The P-vector method seems to have a capability to diagnose the vertical velocity signal.

FIGURE 4 Vertical turning of the P vector: (a) P vector at two different levels, and (b) turning angle (α_{km}) between z_m and z_k, which is the angle between the two horizontal components $P_h^{(m)}$ and $P_h^{(k)}$.

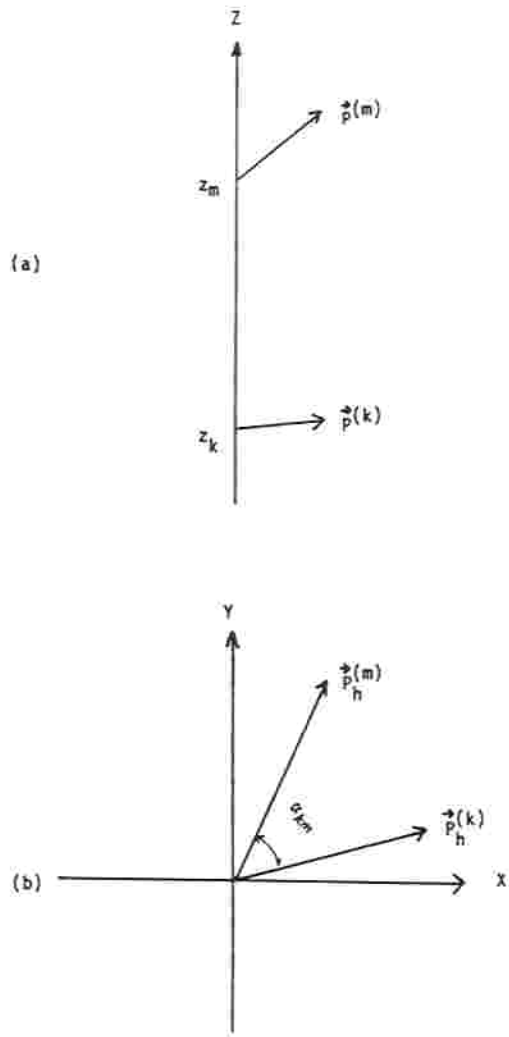

FIGURE 5 Three dimensional velocity (0-th order) at $z = 500$ m: (a) horizontal component $V_h^{(0)}$, (b) vertical velocity w (m/day).

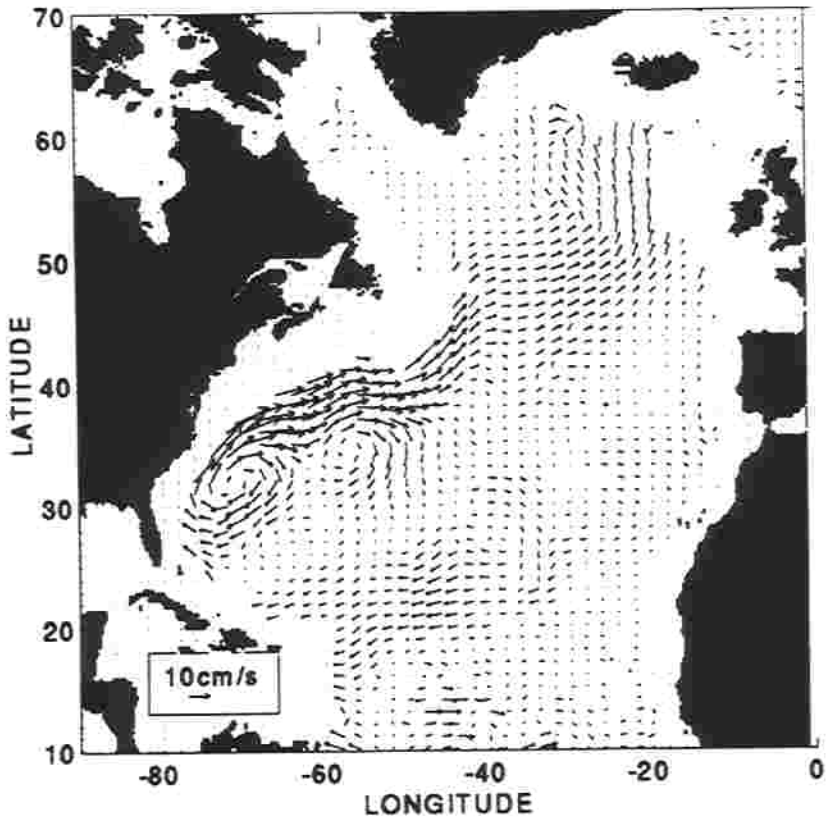

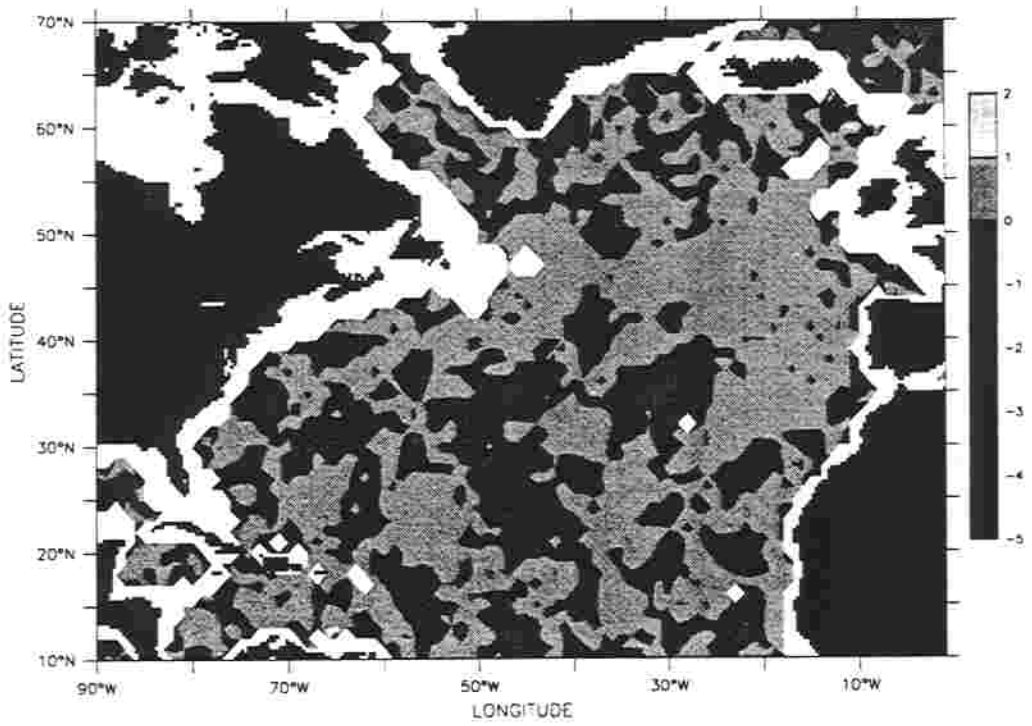

W

FIGURE 6 Absolute velocity vectors at 500 m depth computed by the β spiral method (from: Olbers et al. 1985).

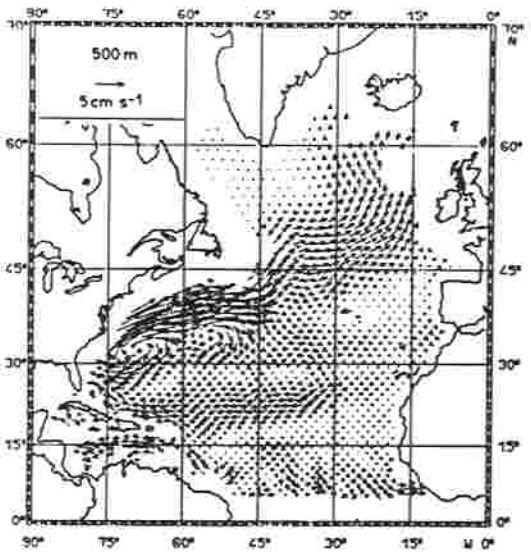

ERROR REDUCTION SCHEME

We refer the velocity field $V^{(0)}$ directly computed from the P-vector to the 0th-order solution. We might ask if the 0th-order solution realistic? We need to check the conservation laws (2) and (4). The computed velocity field contains computational noise due to the truncation errors and data noise due to the instrumentation errors. We use the iteration method to eliminate the noise. Let L denote the iteration step. $L = 0$ refers the velocity field $V^{(0)}$. Is $V^{(0)}$ a good solution? We need to use the local and global conservation indices to verify.

Local and Global Conservation Indices

The errors may lead to a non-conservation of mass and potential vorticity, as measured by

$$R_\rho^{(L)} \equiv |\cos\ \alpha_\rho^{(L)}| = \frac{|V^{(L)} \cdot \nabla\rho|}{|V^{(L)}||\nabla\rho|} \qquad (16a)$$

$$R_q^{(L)} \equiv |\cos\ \alpha_q^{(L)}| = \frac{|V^{(L)} \cdot \nabla q|}{|V^{(L)}||\nabla q|} \qquad (16b)$$

where $\alpha_\rho^{(L)}$ is the angle between $V^{(L)}$ and $\nabla\rho$ $\alpha_q^{(L)}$ the angle between $V^{(L)}$ and ∇q, $R_\rho^{(L)}(x, y, z)$ and $R_q^{(L)}(x, y, z)$ the scaled residues of the density and potential vorticity conservation equations at each point for the L-th iteration. Theoretically, V should be perpendicular to both ∇p and ∇q, i.e.,

$$R_\rho(x, y, z) = 0,\ R_q(x, y, z) = 0$$

for all locations. We define the local conservation index (LCI) as

$$R_c^{(L)}(x, y, z) = R_\rho^{(L)}(x, y, z) + R_q^{(L)}(x, y, z), \qquad (17a)$$

and the global conservation index (GCI) as the average of LCI over the whole domain

$$R_G^{(L)} = \frac{1}{N}\sum\sum\sum R_c^{(L)}(x_i, y_j, z_k), \quad (17b)$$

where N is the total number of the data points.

Local Reference Level

The values of LCI represent the accuracy of the solution at each point (x,y,z). However, the value of GCI denotes the overall accuracy of the solutions. The smaller the values of these indices, the more accurate the velocity field would be. The two parameters LCI and GCI have different usages. LCI is used for picking the local reference level and GCI for necessariness of the next iteration. Starting from the velocity field $V^{(0)}$ obtained from the P-vector method, we check every water column (x_i, y_j), compare LCI vertically, and choose the level with the minimum LCI value

$$R_c(x, y, z_{ref}) = \min_z R_c(x, y, z) \qquad (18)$$

as the reference level for that column. After $z_{ref}(x, y)$ is determined, we can use (1) to recompute the velocity field, $V^{(0)}$, which is called the first iterative velocity.

Iteration Method

Is $V^{(1)}$ better than $V^{(0)}$? We can use *GCI* to compare $V^{(1)}$ and $V^{(0)}$. The condition

$$GCI^{(1)} \geq GCI^{(0)} \qquad (19a)$$

indicates that $V^{(0)}$ is better than $V^{(1)}$. We do not need to do any iteration and choose $V^{(0)}$ as the optimal solution. The condition

$$GCI^{(1)} < GCI^{(0)} \qquad (19b)$$

denotes that the $V^{(1)}$ is better than $V^{(0)}$. We need to pursue a new iteration, i.e., computing $LCI^{(1)}$, in turn determining $z_{ref}^{(1)}$ for $V^{(1)}$ and calculating $V^{(2)}$ by using (1) and $z_{ref}^{(1)}$. Comparison between $GCI^{(2)}$ and $GCI^{(1)}$ leads to a choice if a further iteration is needed (Figure 7). Such an iteration process repeats until no further improvement will be made.

ABSOLUTE VELOCITY AT DIFFERENT DEPTHS

The absolute velocity vectors at different levels are shown in Figure 8. The flow pattern at 100 m level (Figure 8a) is quite similar as that at 500 m level: the Gulf Stream, an anticyclonic subtropical gyre, a weak northern cyclonic gyre. Comparison between Figure 5a and Figure 8a

leads to the fact that the subtropical gyre shrinks in its north-south extension with increasing depth, which agrees with Olbers et al.'s (1985) results.

The flow pattern at deep ocean (2500 m, 3500 m, and 4500 m levels) is shown in Figure 8b-d. The dominant features at 2500 m level (Figure 8b) are the western boundary currents. After passing the Gibbs fracture zone at about 50° *N*, 40° *W* the current splits into two branches: a weak northern branch and strong southern branch. The southern branch flows southwestward, turns westward at 40° *N* 50° *W*, and then follows around the east coast of North America. As this branch enters the Sagasso Sea Trench, a noticeable cyclonic eddy appears at 4500-m level (Figure 8d) to conserve the potential vorticity as the ocean depth increase. The maximum swirl speed is 2 cms^{-1}. After passing 30° *N*, the mid-depth flow at the 2500 m and 3500 m (Figure 8c) levels recirculates northeastward at 30° *N*, 70° *W* with a typical speed 2 cms^{-1}. Different from SS method, our solution does not show a strong southeastward flow near Bahamas carrying water into the South Atlantic Ocean.

A cyclonic-anticyclonic pair is found in the deep water at the eastern (20°-40° W) tropical part (10°-30° *N*) of the North Atlantic Ocean. The cyclonic eddy is in the south, and the anticyclonic eddy is in the north. The maximum swirl speed is around 2 cm/s. This feature is indeed strikingly similar to the map (Defant 1941) of the absolute flow at 2000 m (reproduced by Reid 1981). Furthermore, our computation shows that this dipole structure becomes more evident as the depth increases.

The absolute velocity computed by Olbers et al. (1985) has less noise at the deep level low latitudes than the P-Vector method. This is partly because the turbulence fluxes and associated mixing are neglected in our computation.

ABSOLUTE VELOCITY AT DIFFERENT VERTICAL CROSS SECTIONS

To compare the results from this method with the geostrophic calculation based on the results of the CW method (Wunsch 1978; Wunsch and Grant 1982) and the SS method (Olbers et al. 1985), we display vertical distributions of absolute velocity in latitudinal sections: 57° *W*, 30° *W* (Figure 9) and zonal sections: 24° *N*, 53° *N* and 59° *N* (Figure 10). These figures present the velocity component normal to these sections.

We see some main features in the western (Figure 9a) and eastern parts (Figure 9b) of the subtropical gyre: (a) a strong upper ocean (above 1000 m depth) eastward flow (the Gulf Stream) between 30-40° *N* with a maximum speed greater than 20 cm/s, (b) a weak westward flow below the Gulf Stream (western boundary currents), (c) a near surface westward flow south of 30° *N* (southern branch of the subtropical gyre) with a maximum speed of 6 cm/s, and (d) banded structure in the deep layers (z < -1500 m), where the current direction alternates on a horizontal scale around 2000 km, which is wider than the Wunsch and Grant (1982) results.

We also see some interesting features of the meridional flow at different latitudes (24° *N*, 36° *N*, 53° *N*, 59° *N*), which is summarized as follows. (a) In the upper ocean (above 1000 m), at 24° *N* (Figure 10a) a narrow northward flow appears near the east coast of North America (the Gulf Stream) from 65° *W*-75° *W*,

FIGURE 7 The iteration method for error reduction.

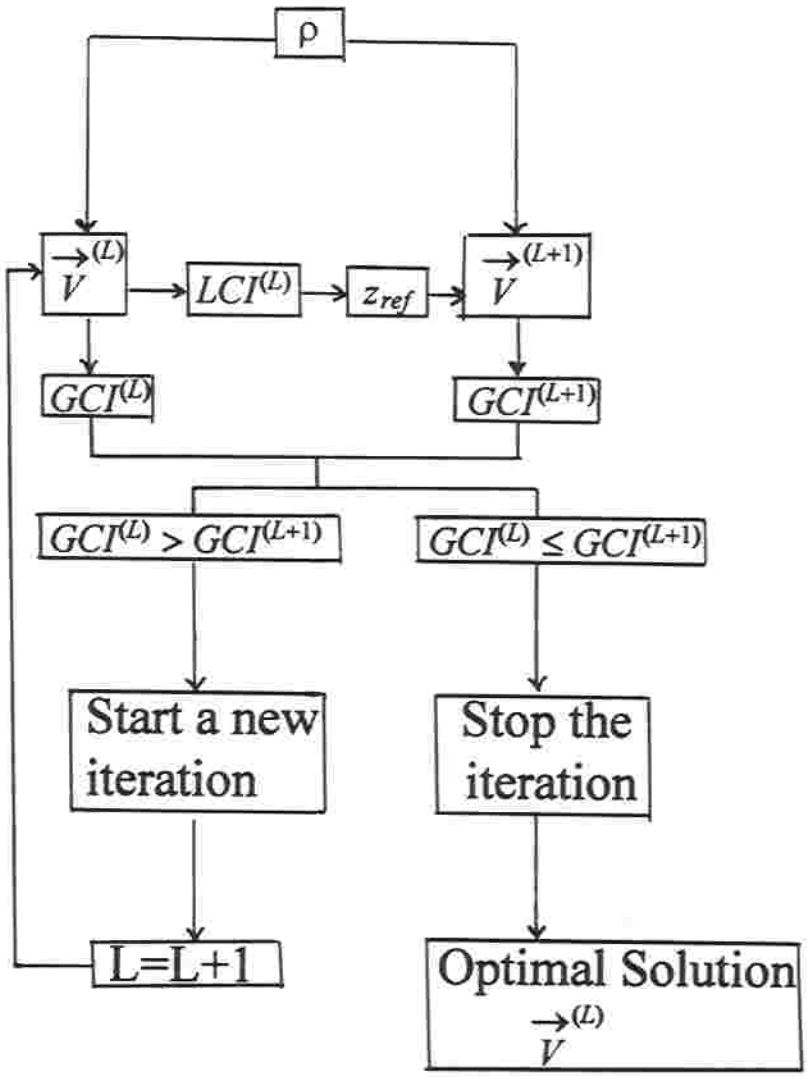

FIGURE 8 Absolute velocity vectors at different levels: (a) 100 m, (b) 2500 m, (c) 3500 m, and (d) 4500 m.

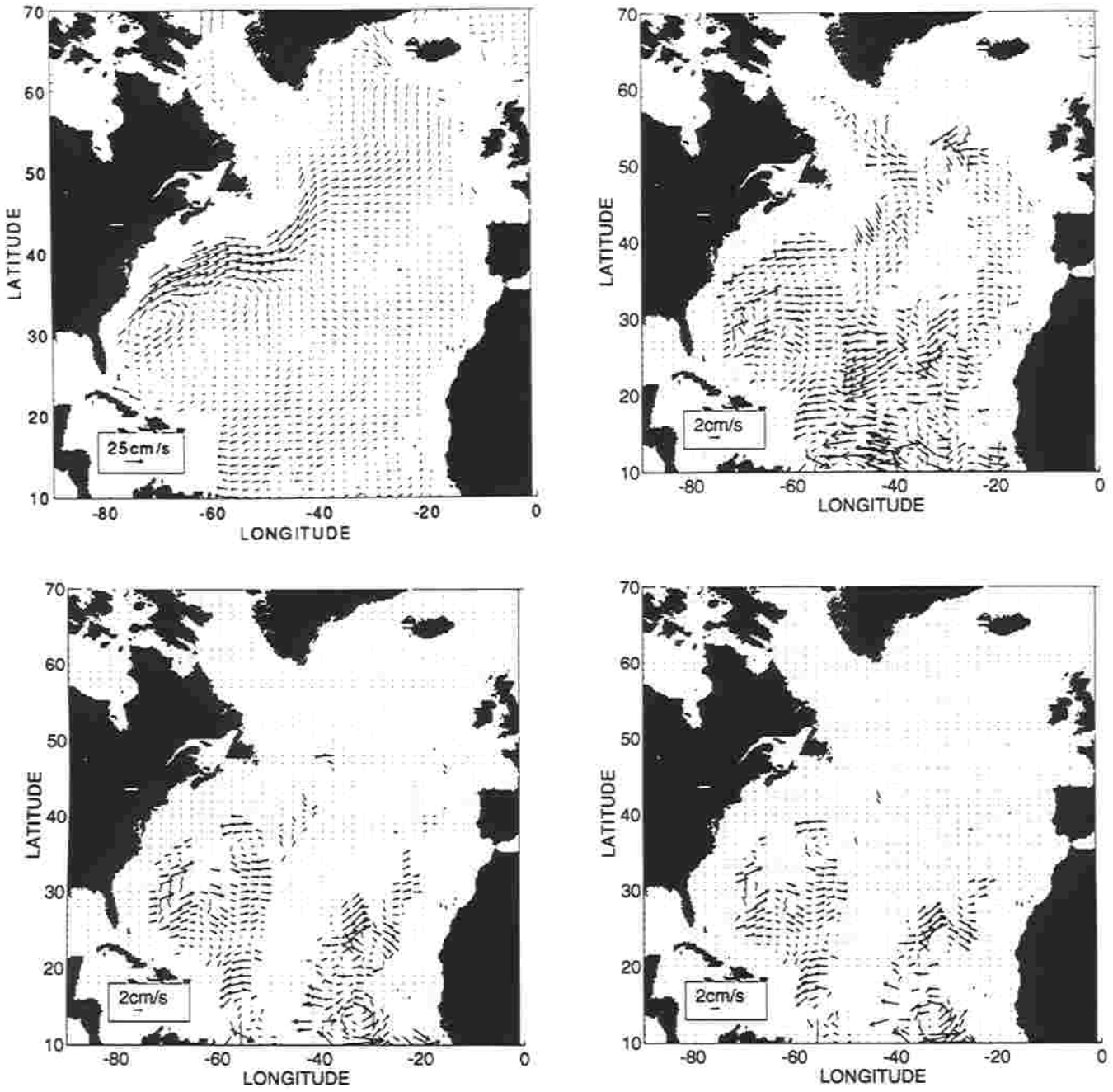

with the maximum speed around 5 cm/s and the width near 1000 km, and a weaker returning southward flow occupies the rest of the region (65° *W*-20° *W*). At the latitude of 36° *N* (Figure 10b), a narrow southward flow appears between 60°-70° *N* and is sandwiched between two northward flows. This indicates the existence of a recirculation cell at that latitude (36° *N*). The core of the northward flow shifts towards east as the latitude increases (Figure 10c and d): the maximum current speed appears between longitudes 20°-30° *W*. (b) In the deeper layer (below 1000 m depth), a banded structure revealing the alternating northward and southward flow with smaller current speed. The width of these alternating bands is around 1000-2000 km, which is also wider than the results of Wunsch and Grant (1982).

FIGURE 9 Absolute zonal velocity (cm/s) along (a) 57° W, and (b) 30° W.

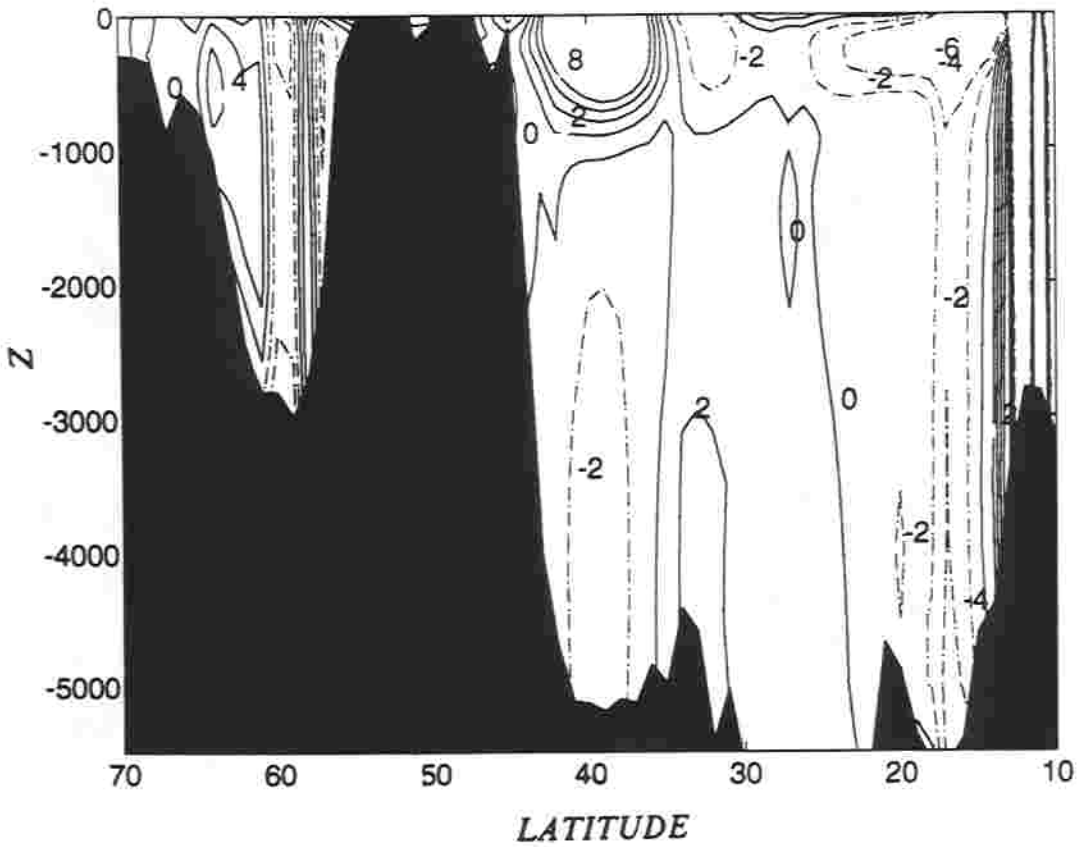

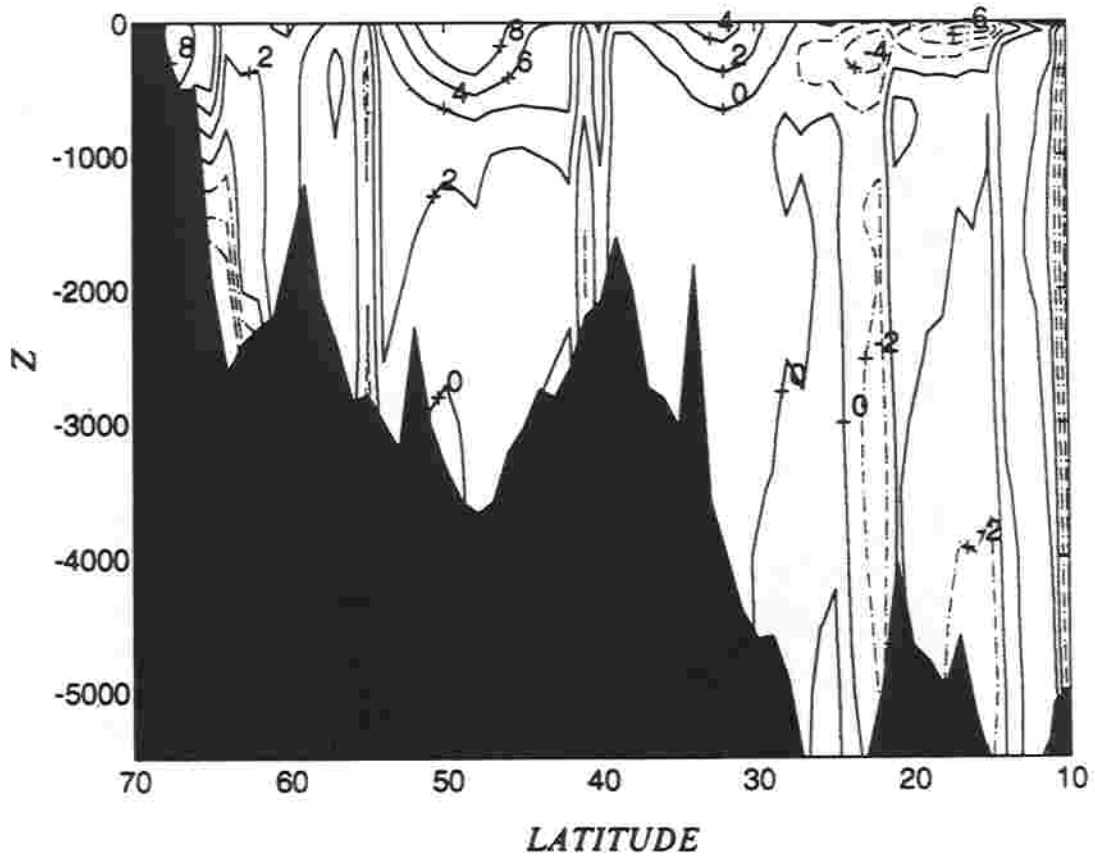

FIGURE 10 Absolute meridional velocity (cm/s) along (a) 24° N, (b) 36° N, (c) 53° N, and (d) 59° N.

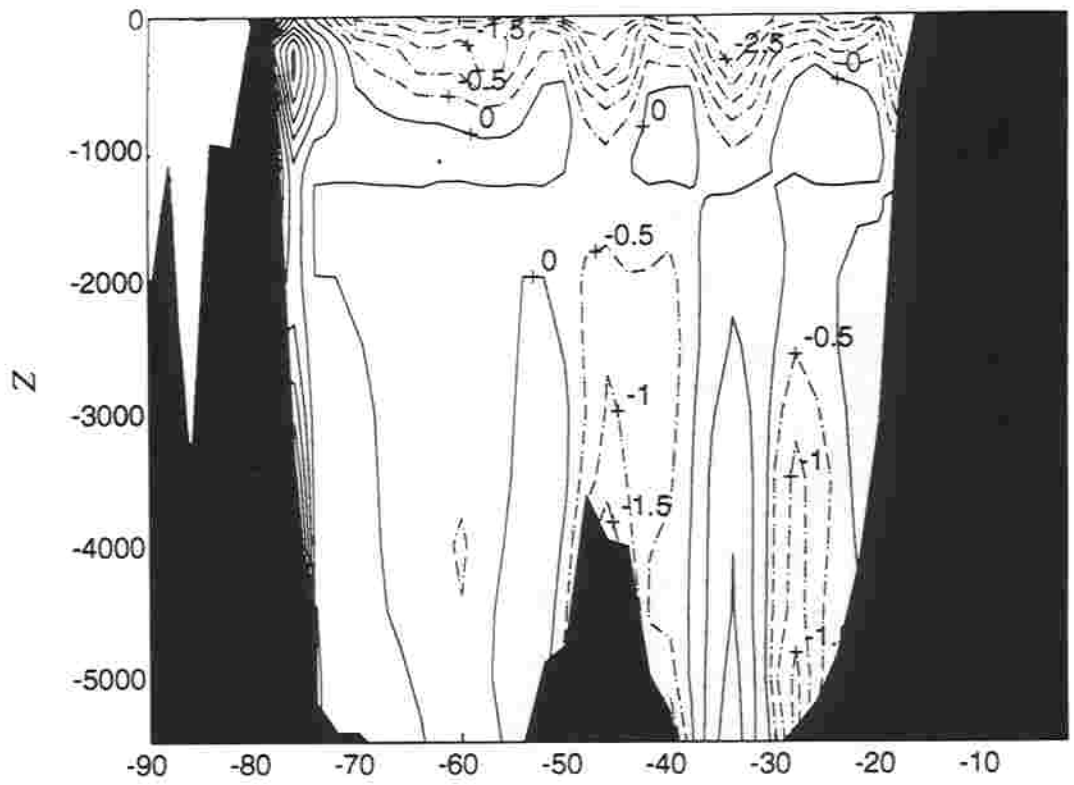

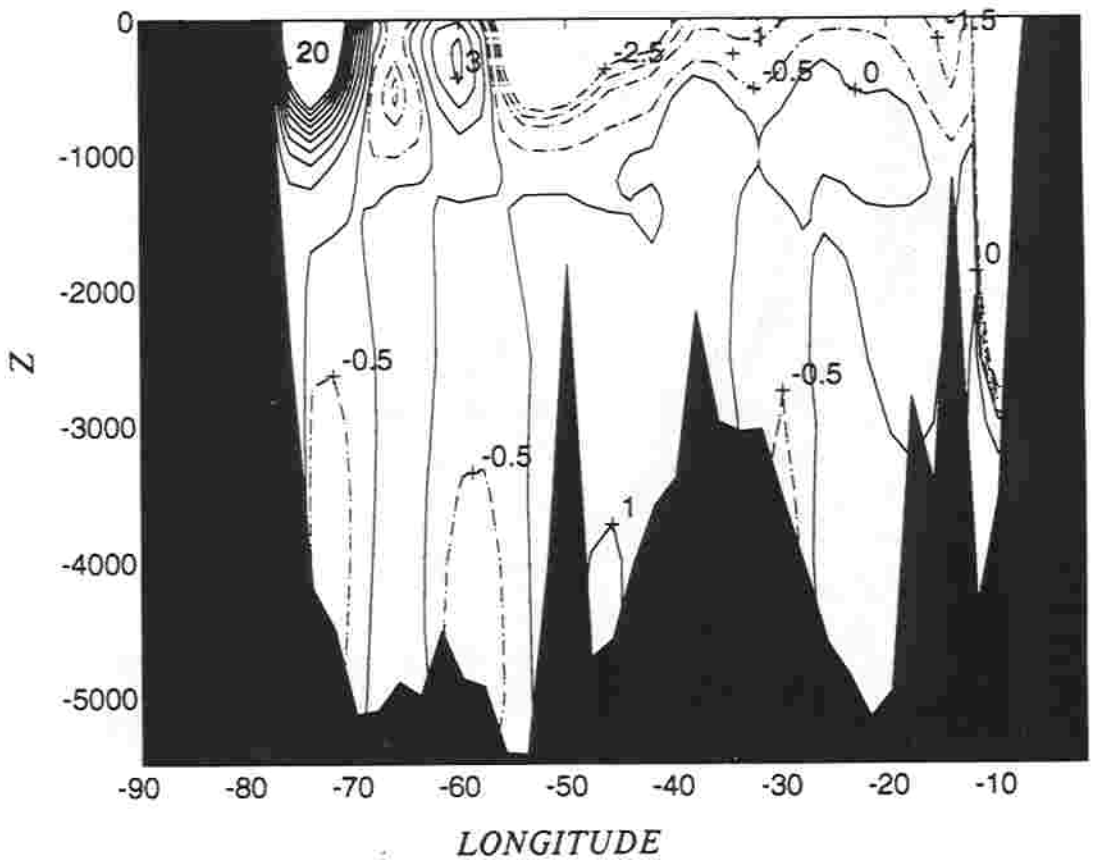

FIGURE 10 Continued

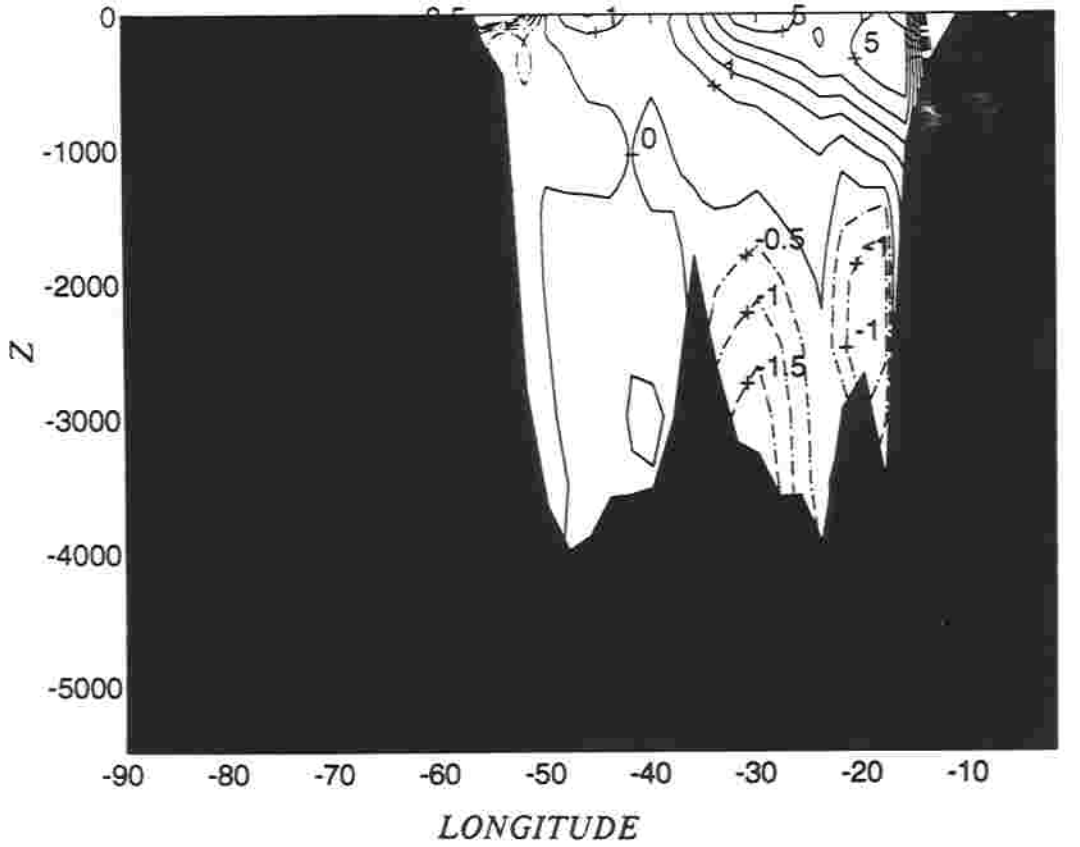

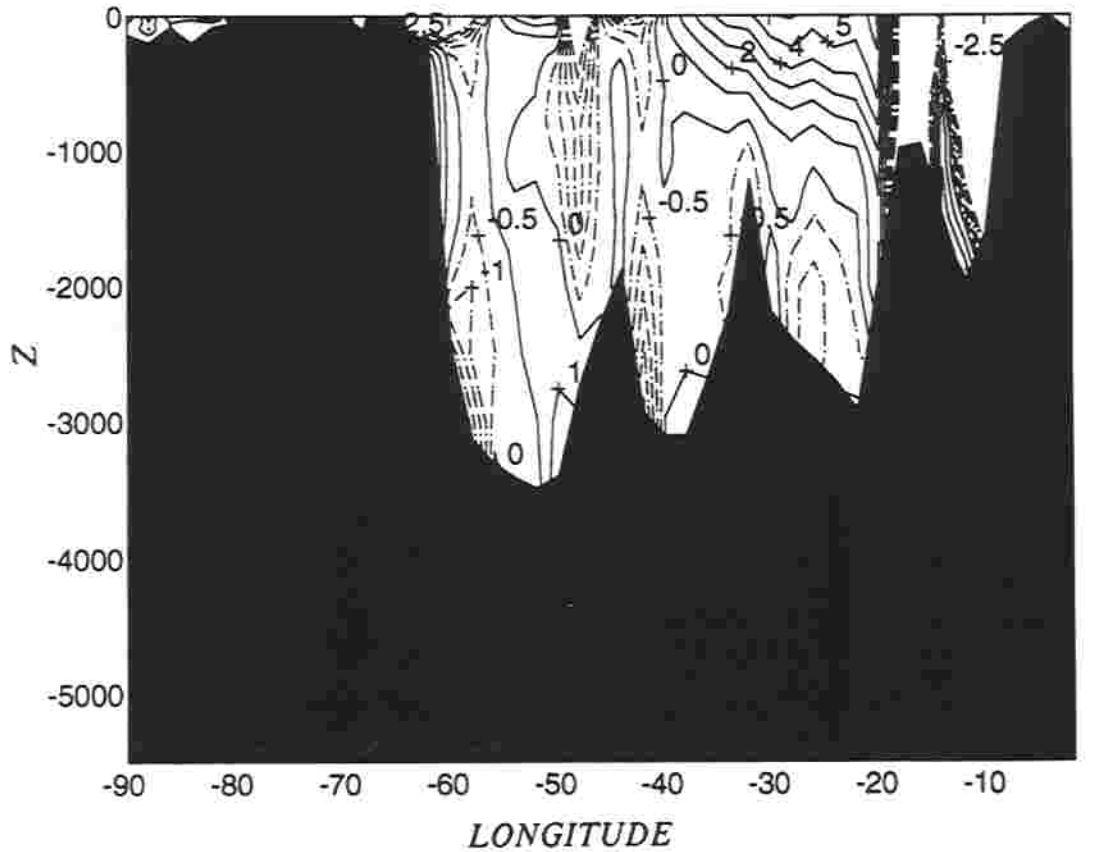

Comparing Figures 9 and 10 with Figure 18a-d in Olbers et al. (1985) and with the results in Wunsch and Grant (1982), we found that our results are closer to the SS method.

CONCLUSIONS

The P-Vector method provides a very simple scheme to compute the absolute velocity from hydrographic data. The resulting circulation pattern resembles the classical view of the North Atlantic circulation (Wust 1935; Defant 1941), especially in the upper ocean. The Physical base of this method is the conservation of potential density and potential vorticity. Therefore, if we use a synoptic hydrographic data set to determine the absolute velocity, we will get better results since a synoptic snapshot of the ocean fields obey the conservation laws.

Similar results were obtained using the P-Vector method, which does not incorporate turbulent mixing and fluxes, and the SS method, which does use turbulent mixing and fluxes (Olbers et al. 1985). Both use the same Levitus data set. This indicates that the main features of the North Atlantic Ocean circulation are determined by the density field rather than by turbulent fluxes and mixing. This supports Pedlosky's idea that the density field itself can determine the main features of the ocean circulation.

The dependence of geostrophic currents on only the density field will lead to a better initialization scheme for ocean numerical models. Ocean numerical models are generally initialized with either observed or climatological temperature and salinity, as well as zero velocities. This leads to an imbalance between the velocity and density fields during the spin-up period. If we use the geostrophic velocity, computed by P-Vector method (from the density field only) instead of zero velocity, as an initial condition for the numerical models, the velocity and density fields are balanced. This might reduce the spin-up time.

ACKNOWLEDGEMENTS

I am grateful to Drs. C. Lozano, M. Carnes, R. Haney, and J. Miller for invaluable discussions. The suggestions and comments from anonymous reviewers are also highly appreciated. This work was funded by the Office of Naval Research NOMP and Physical Oceanography Programs and the Naval Postgraduate School.

REFERENCES

Broecker, W.S. 1991. The great ocean conveyor. *Oceanography*, 4: 79-89.

Bryden, H.L. 1973. New polynomials for thermal expansion, adiabatic temperature gradient and potential temperature gradient of sea water. *Deep-Sea Res.*, 20: 401-408.

Davis, R. 1978. On estimating velocity from hydrographic data. *J. Geophys. Res.*, 83: 5507-5509.

Defant, A. 1941. Quantitative Untersuchungen zu Statik und Dynamik des Atlantischen Ozeans: Die absolute Topographie des physikalischen Meeresniveaus und der Druckflachen sowie die Wasserbewegungen in Raum des Atlantischen Ozeans. *Wiss. Ergeb. Dtsch. Atl. Exped. Meteor 1925-1927, 6, Part 2, 1*, pp. 191-260.

Iselin, C. O'D. 1936. A study of the circulation of the western North Atlantic. *Pap. Phys. Oceanogr. & Meteoro.*, 4, No. 4, 101 pp.

Killworth, P.D. 1986. A Bernoulli inverse method for determining the ocean circulation. *J. Phys. Oceanogr.*, 16: 2031-2051.

Levitus, S. 1982. Climatological atlas of the world ocean. *NOAA Tech. Pap.*, 173 pp.

Needler, G.T. 1985. The absolute velocity as a function of conserved measurable quantities. *Prog. Oceanogr.*, 14: 421-429.

Olbers, D.J., M. Wenzel, and J. Willebrand. 1985. The inference of North Atlantic circulation patterns from climatological hydrographic data. *Rev. Geophys.*, 23: 313-356.

Pedlosky, J. 1986. Thermocline theories. In: *General Circulation of the Ocean*. Ed. H.D.I., Abardanel, and W.R. Young. New York: Springer-Verlag, pp. 55-101.

Reid, J.L. 1978. On the mid-depth circulation and salinity field in the North Atlantic Ocean. *J. Geophys. Res.*, 83: 5063-5067.

Reid, J.L. 1981. On the mid-depth circulation of the world ocean. In: *Evolution in Physical Oceanography*, Ed. B. Warren and C. Wusch. Cambridge, Massachusetts: MIT Press, 70-111.

Schott, F., and H. Stommel. 1978. Beta spirals and absolute velocities in different oceans. *Deep-Sea Res.*, 25:961-1010.

Schmitz, W.J., and M.S. McCartney. 1993. On the North Atlantic circulation. *Rev. Geophys.*, 31: 29-49.

Stommel, H., and F. Schott. 1977. The beta spiral and the determination of the absolute velocity field from hydrographic station data. *Deep-Sea Res.*, 24: 325-329.

Stommel, H., P. Niiler, and D. Anati. 1978. Dynamic topography and recirculation of the North Atlantic. *J. Mar. Res.*, 36: 449-468.

UNESCO. 1981. Tenth report of the joint panel on oceanographic tables and standards. *UNESCO Technical Papers in Marine Sci.* 36, Paris: UNESCO.

Wunsch, C. 1978. The general circulation of the North Atlantic west of 50° W determined from inverse methods. *Rev. Geophys.* 16: 583-620.

Wunsch, C. and B. Grant. 1982: Towards the general circulation of the North Atlantic Ocean. *Prog. Oceanogr.*, 11: 1-59.

Wust, G. 1935. Schichtung und Zirkulation des Atlantischen Ozean: Das Bodenwasser und die Stratosphare, *Wiss. Ergeb. Dtsch. Atl. Exped. Meteor 1925-1927, 6*, 288p.